Numerical study of the influence of wall roughness on laminar boundary layer flashback

Shuyu Ding [1,*] Kai Huang,[1,2,*] Yifan Han,[1,2] and Damir Valiev [1,2,3,†]
[1]*Department of Energy and Power Engineering, Tsinghua University, Beijing 100084, China*
[2]*Center for Combustion Energy, Tsinghua University, Beijing 100084, China*
[3]*Key Laboratory for Thermal Science and Power Engineering of Ministry of Education, Tsinghua University, Beijing 100084, China*

(Received 17 August 2020; accepted 11 February 2021; published 24 February 2021)

Modification of flow characteristics by wall roughness has been intensively analyzed in the field of fluid mechanics. However, few studies have considered wall roughness in boundary layer flame flashback. In the present study, laminar boundary layer flashback in channels with roughness at the walls is studied using two-dimensional simulations. The laminar premixed flame interacts with a linear shear flow along a wall with triangle-shaped fine roughness. The simulation results show that wall roughness in this configuration can attenuate flashback tendency due to enhanced heat loss to the boundary. By comparing results for isothermal and adiabatic boundary conditions at the walls, it is shown that the heat loss enhancement due to wall roughness may be a dominant effect in determining flame propagation characteristics for the walls with low thermal resistance. The critical velocity gradient is shown to decrease with wall roughness level and increase with thermal gas expansion ratio.

DOI: 10.1103/PhysRevFluids.6.023201

I. INTRODUCTION

As global warming and environmental pollution become global issues, clean combustion is receiving special attention in both research and industry. Out of all the clean combustion technologies, H_2 lean premixed combustion is among the most promising ones as it can help to drastically reduce CO_2 and NO_x emissions [1]. However, this technology is susceptible to flame instabilities and combustion safety issues. Among others, solving flashback issues has become the bottleneck problem for its wide application. When flow rates are high, the velocity of the flame is generally much lower than that of the premixed gas in the central part of the channels or tubes; flashback is largely restrained in this area. Therefore, flashback in boundary layers becomes the most important issue. The theoretical study of boundary layer flashback was pioneered by Lewis and von Elbe [2]. A large number of subsequent studies have looked into this problem experimentally, theoretically, and numerically [3–11]. Most of the studies focus on flammable gas properties and flow characteristics to describe flashback tendency. Flashback limits of laminar premixed flames are shown to be significantly dependent on the Lewis number of the fuel mixture [6]. It is also known that thermal

*These authors contributed equally to this work.
†dvaliev@tsinghua.edu.cn

gas expansion plays a crucial role in boundary layer flashback dynamics for turbulent premixed flames [8,9].

So far, little light has been shed on the influence of the wall boundary conditions on flashback. In experiments by Eichler *et al.* [12], channels equipped with ceramic tiles were used, and their influence on the quenching gap was discussed. Kurdyumov *et al.* [5,6] studied the effect of variable heat loss at the smooth wall on laminar flame flashback. In recent years, increasingly more studies have addressed the effects of wall roughness on the reacting flows. Wakisaka and colleagues [13] conducted experiments in engines and showed that using thermal insulation materials at the walls would increase thermal efficiency, while increased wall roughness would significantly influence spray combustion. Also, in detonation studies, the influence of wall roughness on detonation properties is a field of active research [14]. However, there are relatively few works on the effects of wall roughness on boundary layer flashback. Recently, both nonreacting numerical simulations and flame flashback experiments were used to study the influence of streamwise roughness on flashback [15,16]. The results suggest that roughness can effectively reduce boundary layer flashback by reducing drag force.

Systematic studies of the influence of the wall boundary conditions on nonreacting flow, with focus on both flow characteristics and heat loss, have been conducted over the years. Tuck and Kouzoubov [17] analytically studied rough boundary conditions in laminar flow and concluded that roughness would lift the flow and thus change its momentum. Turgay and Yazicioglu [18] conducted simulation of a flow in a channel with a rough wall and compared the results with the case where the wall is smooth, concluding that roughness can increase local heat losses.

So far, the effect of fine wall roughness on flame flashback has not been studied either numerically or experimentally. In the present study, two-dimensional numerical simulations are employed to study the effects of fine roughness placed perpendicular to the flame propagation direction. The effects of wall roughness and thermal gas expansion on critical velocity gradients and flashback speeds are scrutinized. The analysis is focused on the effect of wall roughness on the modification of the oncoming flow and quenching gap in the near-wall region. Lewis and von Elbe's [2] critical gradient model is revisited for the case of fine wall roughness.

This paper consists of four sections. Details of numerical simulation are presented in Sec. II. In Sec. III, simulation results and their analysis are presented, followed by the Conclusions.

II. DETAILS OF NUMERICAL SIMULATION

Two-dimensional Cartesian hydrodynamic and combustion equations that include transport processes (thermal conduction, diffusion, and viscosity) and the Arrhenius chemical kinetics are solved in the numerical simulations. In tensor form, the governing equations read

$$\frac{\partial \rho}{\partial \mathrm{t}} + \frac{\partial}{\partial x_i}(\rho u_i) = 0, \tag{1}$$

$$\frac{\partial}{\partial \mathrm{t}}(\rho u_i) + \frac{\partial}{\partial x_j}(\rho u_i u_j + \delta_{ij} P - \tau_{ij}) = 0, \tag{2}$$

$$\frac{\partial}{\partial \mathrm{t}}\left(\rho\varepsilon + \frac{1}{2}\rho u_i u_j\right) + \frac{\partial}{\partial x_i}\left(\rho u_i \bar{h} + \frac{1}{2}\rho u_i u_j + q_i - u_j \tau_{ij}\right) = 0, \tag{3}$$

$$\frac{\partial}{\partial \mathrm{t}}(\rho Y) + \frac{\partial}{\partial x_i}\left(\rho u_i Y - \frac{\mu}{Sc}\frac{\partial Y}{\partial x_i}\right) = -\frac{\rho Y}{t_R}\exp\left(-\frac{E_a}{R^0 T}\right), \tag{4}$$

where Y is the fuel mass fraction, $\varepsilon = QY + C_V T$ the internal energy, $\bar{h} = QY + C_p T$ the enthalpy, Q the chemical energy release, and C_V and C_P the heat capacities at constant volume and pressure,

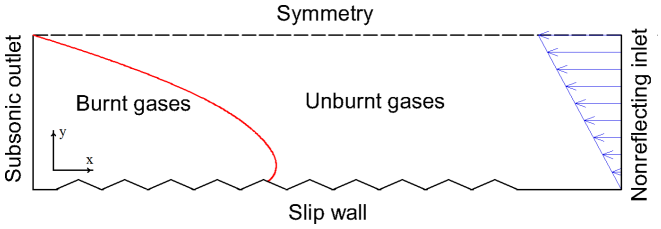

FIG. 1. A sketch of the numerical configuration.

respectively. The stress tensor τ_{ij} and the energy diffusion vector q_i are

$$\tau_{ij} = \mu\left(\frac{\partial u_i}{\partial x_j} + \frac{\partial u_j}{\partial x_i} - \frac{2}{3}\frac{\partial u_k}{\partial x_k}\delta_{ij}\right), \tag{5}$$

$$q_i = -\mu\left(\frac{C_P}{\mathrm{Pr}}\frac{\partial T}{\partial x_i} + \frac{Q}{\mathrm{Sc}}\frac{\partial Y}{\partial x_i}\right), \tag{6}$$

where μ is the dynamic viscosity, and Pr and Sc the Prandtl and Schmidt numbers, respectively. To rule out the effect of thermal-diffusive instability, we take the unity Lewis number, with Prandtl and Schmidt numbers $\mathrm{Pr} = \mathrm{Sc} = 0.75$, and dynamic viscosity $\mu = 1.7 \times 10^{-5}\,\mathrm{N\,s/m^2}$. Without the loss of generality of the results, the following common approximations are used [19–21]: The model fuel-air mixture and burnt gas are assumed to be perfect gases with a constant molar mass $m = 2.9 \times 10^{-2}\,\mathrm{kg/mol}$, with $C_V = 5R^0/2m$, $C_P = 7R^0/2m$, i.e., the adiabatic index $\gamma = C_P/C_V = 1.4$, and the equation of state,

$$P = \frac{\rho R^0 T}{m}, \tag{7}$$

where $R^0 \approx 8.31\,\mathrm{J/(mol\,K)}$ is the universal gas constant. We consider a single-step irreversible Arrhenius reaction of the first order with an activation energy E_a and a characteristic time t_R. The initial density, pressure, and temperature were taken as $\rho_0 = 1.16\,\mathrm{kg/m^3}$, $P_0 = 10^5\,\mathrm{Pa}$, and $T_0 = 300\,\mathrm{K}$, respectively. The thermal expansion factor is taken in the range $\Theta \equiv \rho_b/\rho_0 = 6 - 10$, where ρ_b is the burnt gas density. The range covers gas expansion factors typical for hydrocarbon and hydrogen burning. The energy release in the reaction is therefore quantified as $Q = C_P T_0(\Theta - 1)$.

A characteristic constant of time dimension t_R in the irreversible Arrhenius reaction is adjusted to obtain a particular value of the laminar flame speed S_L by solving the associated eigenvalue problem. The diffusive flame thickness is a parameter of length dimension conventionally defined as $\delta_L = \mu/\,\mathrm{Pr}\,\rho_0 S_L$ [19,20]. It is noted that a thermal flame thickness, calculated using the maximum temperature gradient, would be several times higher as compared to δ_L for the same laminar flame structure [8]. The activation energy is taken as $E_a/\Theta R^0 T_0 = 4$, and initial flame propagation Mach number is $\mathrm{Ma} = S_L/c_0 = 0.001$, where c_0 is the speed of sound in the fuel mixture. The fixed channel half width $50\delta_L$ was chosen to ensure the absense of the global flow reversal generated by the flame based on the series of additional test simulations for different channel widths. The free-slip adiabatic and isothermal boundary conditions are employed at the roughness elements. A sketch of the numerical setup is presented in Fig. 1. At the nonreflecting inlet, a linear velocity profile is applied, starting from zero velocity at the bottom wall and attaining maximum velocity at the upper boundary of the domain; see Fig. 1. At the left channel end the boundary condition is set as subsonic outflow. The inlet velocity gradient $g = \frac{dU}{dy}$ is kept constant throughout each simulation run and varied in the range $(0.1 - 0.2)S_L/\delta_L$ between different simulations.

TABLE I. Resolution test results for different cell size l, at $\Theta = 8$, $g = dU/dy = 0.1\, S_L/\delta_L$, $k = 1$.

l/δ_L	U_{tip}/S_L	$\Delta U_{\text{tip}}/U_{\text{tip}}$
0.4	0.2248	N/A
0.2	0.2490	10.77%
0.1	0.2564	2.971%
0.05	0.2590	1.014%

The initial flame structure was set as

$$T = T_f + T_f(\Theta - 1)\exp\left[-\frac{\sqrt{(x - r_f)^2 + (y - r_f)^2}}{\delta_L}\right], \quad \text{if} \quad x^2 + y^2 > r_f^2, \tag{8}$$

$$T = \Theta T_f, \quad \text{if} \quad x^2 + y^2 < r_f^2, \tag{9}$$

$$Y = \frac{\Theta - T/T_f}{\Theta - 1}, \quad \mathrm{P} = P_f, \quad \boldsymbol{u} = 0. \tag{10}$$

Here, r_f is the radius of the high-temperature sector-shaped area specified at the left bottom corner of the channel to ignite the initial flame kernel.

The two-dimensional (2D) compressible Navier-Stokes solver used here was previously successfully utilized in studies of laminar flames, hydrodynamic combustion instabilities, flame acceleration [19–21], and related phenomena, as well as aeroacoustic applications [22,23]. The solver is based on the cell-centered finite-volume method, which is second-order accurate in time, up to fourth-order accurate in space for the convective terms, and second-order accurate in space for the diffusive terms.

We performed a set of resolution tests, in which flame tip velocities $U_{\text{tip}} = \frac{dx^*}{dt^*}$ were compared for different cell sizes l, where $x^* = \frac{x}{\delta_L}$, $t^* = t\frac{S_L}{\delta_L}$. Table I shows the summary of the convergence tests for the steady flame velocity U_{tip} at decreasing grid spacing l. Based on the resolution tests, a uniform grid with the quadratic cells of size $0.2\delta_L$ was used in this work to ensure proper resolution of a curved flame. It is also noted that a small oscillation of a flame tip velocity is observed for all cases. This is due to the minor change of flow properties around the roughness elements that would be reflected in flame tip velocity. In the present work, the locally weighted scatterplot smoothing (LOWESS) method is used to smooth out this effect for a better presentation of results.

Triangle-shaped roughness is chosen for its simplicity and ease of implementation using nonorthogonal structured mesh. We define the ratio of the height h to the half length s of the base of a roughness element as the slope k, as illustrated in Fig. 2. The base of the roughness array is located at $y = 0$. Fine roughness is specified by setting s to $0.4\delta_L$, with h varying in the range 1–4 s. Since s is fixed, k would effectively define the vertical size of a roughness element, which, in turn, would affect the wall surface area per unit length of the channel. By specifying multiple layers of parallelogram-shaped grids, we ensured the gradual change of cell size in the vicinity of

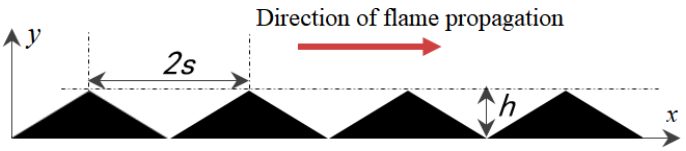

FIG. 2. A sketch of the roughness element configuration.

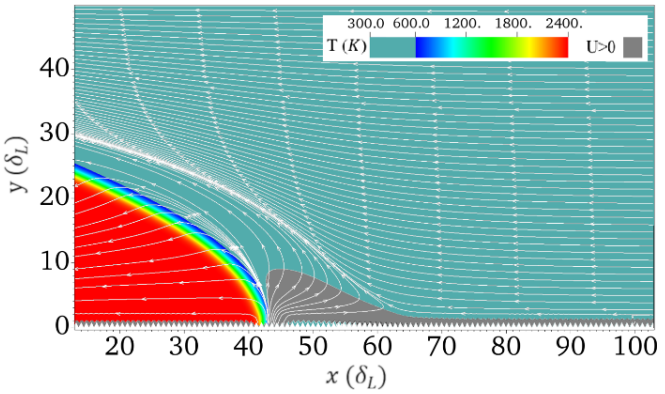

FIG. 3. Temperature field and backflow region for adiabatic walls. $\Theta = 8$, $g = \frac{dU}{dy} = 0.1S_L/\delta_L$, $k = 4$.

the boundary with roughness. To further improve the flow stability near the inlet and outlet, several layers of quadratic grids with uniform size are posted at the areas adjacent to domain corners. In the resolution tests of Table I, the number of cells per roughness face varied from 1 to 8. Spatial resolution of the production simulation runs corresponds to two cells per roughness face.

III. RESULTS AND DISCUSSIONS

A. Influence of wall roughness on flashback speed

Wall roughness is expected to have a twofold effect on the flashback tendency: On one hand, change of the roughness element height would affect the flow [17]; on the other hand, the heat loss to the wall is going to be modified through the change of the surface area (and, consequently, heat flux) per unit length of the channel. In order to get a deeper insight into both effects, we first deliberately neglect the heat loss effect by specifying adiabatic thermal boundary conditions at the wall. In the initial auxiliary study with an adiabatic wall we focus on the flow modification and its effect on the flame dynamics in the absence of quenching at the wall. In the previous systematic studies of wall roughness on flashback [15,16], the propensity of flashback was estimated based on the analysis of flow modification by wall roughness using nonreacting flow simulations. To further assess the predictive capability of such approach, we perform reactive simulations with and without heat loss at the walls. It is realized that in reality heat loss and flame quenching at the wall are inevitable; thus, the adiabatic wall is a limiting case of infinitely large thermal resistance of the wall. Next, we study a more realistic case with heat loss at the wall by considering the isothermal wall boundary condition.

Under the adiabatic boundary condition, four sets of numerical simulation for roughness slopes $k = 1, 2, 3, 4$ were performed. The thermal expansion factor Θ was constant, $\Theta = 8$, and the inlet velocity gradient g was $0.1S_L/\delta_L$. After a short transitional period upon ignition, the flame would propagate upstream with a steady velocity U_{tip} (measured as velocity of the flame tip in the laboratory frame) in all cases with adiabatic walls. A representative flame shape is shown in Fig. 3, where the combined temperature and velocity field is presented, with backflow indicated by the darker gray shade. Formation of the backflow region, as well as upstream flame propagation, were observed in all cases with adiabatic walls. In Fig. 4, the steady flame tip velocity U_{tip} and stagnation zone thickness H_{stag} are presented for different roughness slopes k. The near-wall zone where the value of absolute flow velocity is no larger than $0.1S_L$ is defined as the stagnation zone, with corresponding height H_{stag} [illustrated in Fig. 5 (bottom)]. As can be seen from Fig. 4, as the roughness slope k increases, the flame propagation speed U_{tip} increases as well. In other words,

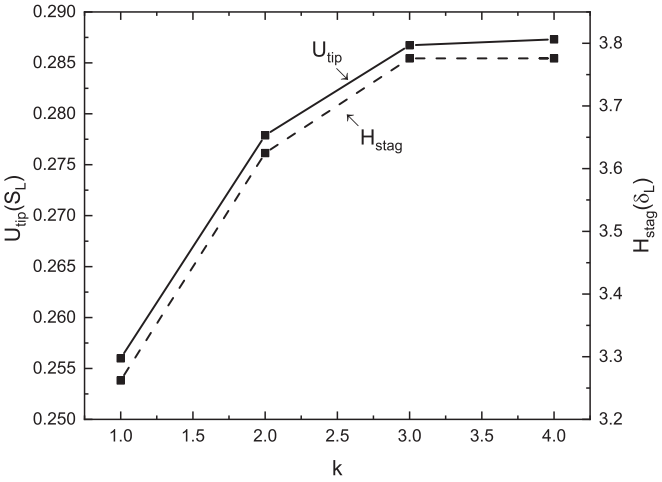

FIG. 4. Stationary flame tip velocity U_{tip} and stagnation zone thickness H_{stag} for different roughness slopes k. Adiabatic walls, $\Theta = 8$, $g = \frac{dU}{dy} = 0.1 S_L/\delta_L$.

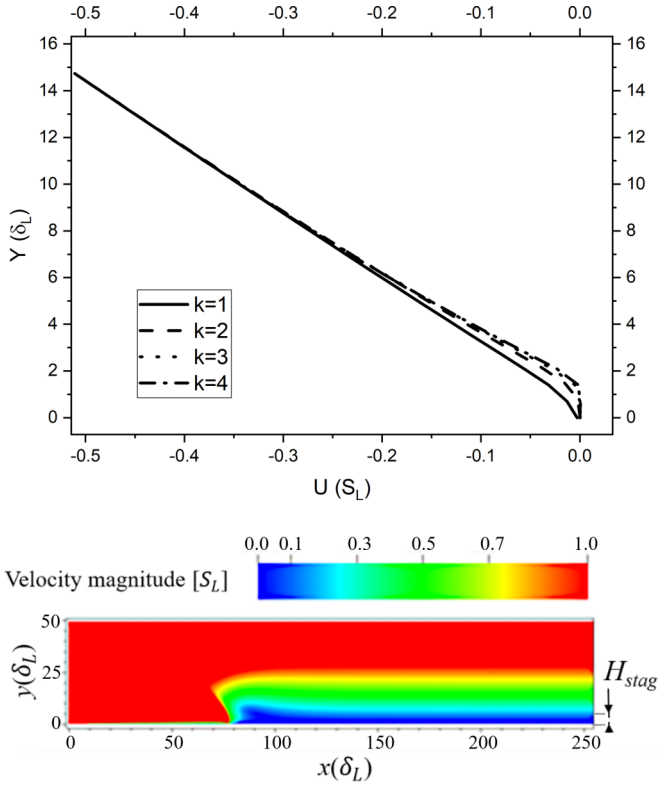

FIG. 5. (Top) Vertical cross sections of horizontal component U of flow velocity ahead of the flame for different k. $\Theta = 8$, $g = \frac{dU}{dy} = 0.1 S_L/\delta_L$, $k = 1, 2, 3, 4$. (Bottom) Velocity magnitude for $k = 1$. Upper threshold of $1 S_L$ is applied to visualize the near-wall region. Stagnation zone thickness H_{stag} corresponds to $0.1 S_L$.

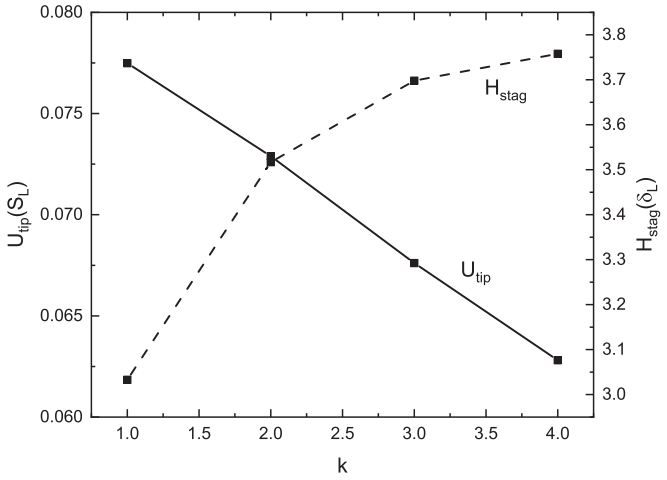

FIG. 6. Stationary flame tip velocity U_{tip} and stagnation zone thickness H_{stag} for different roughness slopes k. Isothermal walls, $\Theta = 8$, $g = \frac{dU}{dy} = 0.1 S_L/\delta_L$.

roughness under the adiabatic condition appears to promote boundary layer flashback. For $k = 3$ and $k = 4$, the flame velocity reaches its maximum value.

The cross-section velocity profiles for the four cases ($k = 1-4$) are illustrated in Fig. 5 (top), where the horizontal component U of flow velocity ahead of the flame is plotted. Figure 5 (bottom) provides an illustration of the stagnation zone thickness H_{stag}. It is noted that, in a given simulation, the cross-section velocity profiles are the same for all axial locations between the flow reversal ahead of the flame (Fig. 3) and the channel inlet, i.e. the cross-section velocity profile remains constant as flow travels from the inlet towards the flame, except for a quick modification at the roughness elements close to the inlet. From Figs. 4 and 5 it is seen that with the increase of roughness slope, the stagnation zone thickness H_{stag} increases too, in a strong correlation with the change of flame propagation speed U_{tip}. This indicates that wall roughness can promote boundary layer flashback along an adiabatic wall through the increase of stagnation layer thickness, effectively lifting the flow above the wall surface, in accordance with earlier studies [17]. Since there is no flame quenching along the wall in the case of an adiabatic boundary, the upstream flame propagation is facilitated for the larger stagnation layer thicknesses due to lower oncoming flow velocity in the near-wall region, that would otherwise more strongly counteract the flame propagation.

Under the more realistic isothermal boundary condition, the parametric study is focused on varying the thermal gas expansion Θ and roughness slope k. As shown in Fig. 6, with the increase of roughness slope k, the flame propagation speed decreases. In other words, the present results indicate that roughness may help to reduce the risk of boundary layer flashback when the heat loss is high, i.e., in most practical situations with low thermal resistance of the walls. This is in line with the experimental results for the streamwise placed roughness [15,16]; at the same time, the tendency for the flashback velocity is the opposite to that of the adiabatic wall case presented above. The dependence of stagnation zone thickness H_{stag} and flame tip velocity U_{tip} on k for the isothermal wall is shown in Fig. 6. It can be seen that as the roughness slope increases, the stagnation zone thickness H_{stag} increases as well, just as in the adiabatic case. However, the trend for the flame tip velocity U_{tip} is reversed as compared to the adiabatic case. Moreover, as can be seen from Figs. 4 and 6, for the same roughness slopes, the stagnation layer thickness is nearly the same for both the isothermal and adiabatic wall. It indicates that for the fine roughness, the heat loss at the wall may have a stronger impact on flashback tendency than the momentum loss. Larger specific surface area (per unit length of the channel) results in larger heat loss, which increases the flame quenching gap in the near-wall region. Lewis and von Elbe's model [2] predicts that, as the quenching gap and

penetration distance are increasing, the flame tip propagation is going to be counteracted by a larger oncoming flow velocity, which would result in a lower flame propagation speed, in agreement with the present results.

The latter scenario is expected to be relevant in most realistic situations when the wall thermal resistance is low (e.g., for metal walls), and the elements of roughness could be effectively cooled down. In such situation, roughness size would be enhancing the overall heat loss. In principle, walls with very high thermal resistance may be to some extent approximated by the adiabatic boundary condition. Recent studies [24] showed that quartz tubes (i.e., those with higher thermal resistance) generally yielded a higher flashback propensity than that of metal tubes that have lower thermal resistance. Present results indicate that the importance of roughness in flashback may be higher when heat loss to the wall is strong. In that case, evaluating flashback tendency based on sole measurements of flow characteristics in nonreacting gases and comparison with estimated quenching distances measured for the smooth walls (an approach that was adopted in, e.g., [15,16]) may not be always representative, since quenching distance may be affected by roughness.

B. Critical velocity gradients

To further investigate the influence of wall roughness on boundary layer flashback propensity, we quantify the critical velocity gradients for different roughness slopes k and thermal expansion factors Θ, and verify the applicability of the critical velocity gradient model [2] for the walls with roughness. By fixing both k and Θ, and varying the inlet velocity gradient, the critical value of the inlet velocity gradient g_c, at which the flame will experience blow out, can be found using the bisection approach. A standard "phone-book look-up" type search is executed, where we first bracket the value of g_c by identifying the two inlet velocity gradients g_1 and g_2; one is when the flame is propagating upstream ($g_1 < g_c$), and the other one is when the flame is blown out ($g_2 > g_c$). Next, we perform a simulation with inlet velocity gradient $g = (g_1 + g_2)/2$, obtain either upstream flame propagation or flame blowout, and repeat the bracketing iteration, until the critical velocity gradient is identified for which the flame position is (nearly) steady; i.e., the flame is stabilized at certain position in the channel by the oncoming flow.

Three sets of simulations are conducted for the thermal expansion factors $\Theta = 6$, 8, and 10, in order to gain insight into how the influence of the wall roughness on the critical velocity gradient would change with thermal gas expansion. The values of the critical velocity gradient g_c obtained in these three sets of runs are presented in Fig. 7. It is seen from Fig. 7 that the critical velocity gradient g_c decreases with the increase of roughness slope k. The observed trend for g_c is consistent with the flame propagation velocity trend for the isothermal walls from Sec. III A. For a given k, increase of the gas expansion Θ leads to the increase of the critical gradient g_c. This result indicates that the volumetric gas expansion at the flame front can impact the flame-flow interaction in boundary layer flashback, and promote the upstream flame propagation, which is consistent with the studies of gas expansion effects on flame dynamics in channels [20], and of the flame interaction with periodic shear [25]. The present results confirm the important role of thermal gas expansion in boundary layer flashback dynamics [8,9,25].

The temperature fields and streamlines at the critical condition for $\Theta = 8$ and two different $k = 1$, 4 are shown in Figs. 8 (left) and 9 (left). The corresponding fields of reaction rate (scaled by maximum value) are presented in Figs. 8 (right) and 9 (right), where the increase of the quenching distance is visible for $k = 4$, as compared to $k = 1$. Results of Fig. 5 indicate that wall roughness modifies the flow in the near-wall area; however, the flow modification at the wall cannot alone explain the decrease of the critical velocity gradient (Fig. 7) with the increase of k. Heat loss, as a dominant process in forming the quenching gap [26], is also dominating the critical condition for flashback. Similar to Sec. III A, we can apply the model of Lewis and von Elbe to explain this trend: As the penetration distance increases, the velocity balance between the flame tip velocity and oncoming flow velocity at the quenching distance is modified, resulting in a different critical gradient [2]. It is noted that channel walls are neither adiabatic nor isothermal in practical reality, but

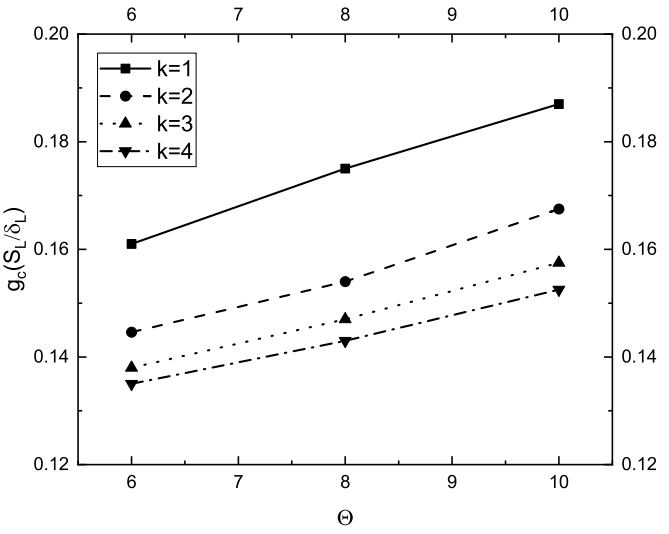

FIG. 7. Critical inlet velocity gradient (for isothermal walls) versus thermal expansion Θ for different k.

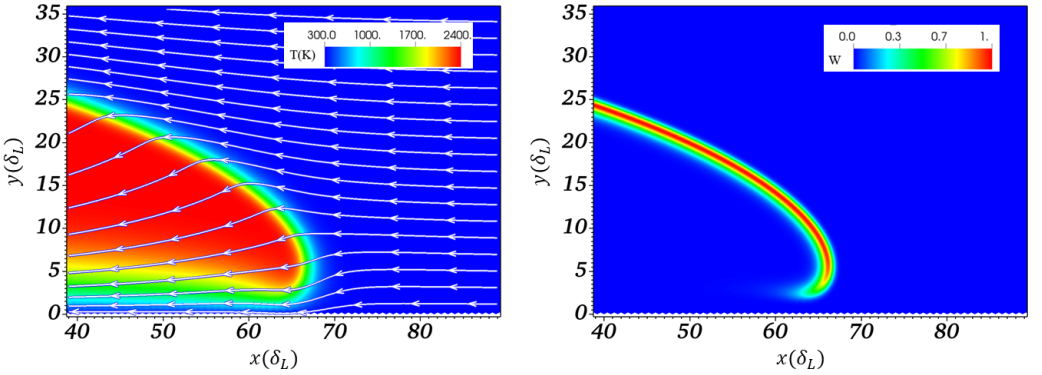

FIG. 8. (Left) Temperature field and streamlines, and (right) scaled reaction rate field, under critical condition. Isothermal wall, $\Theta = 8$, $g = \frac{dU}{dy} = 0.175 S_L/\delta_L$, $k = 1$.

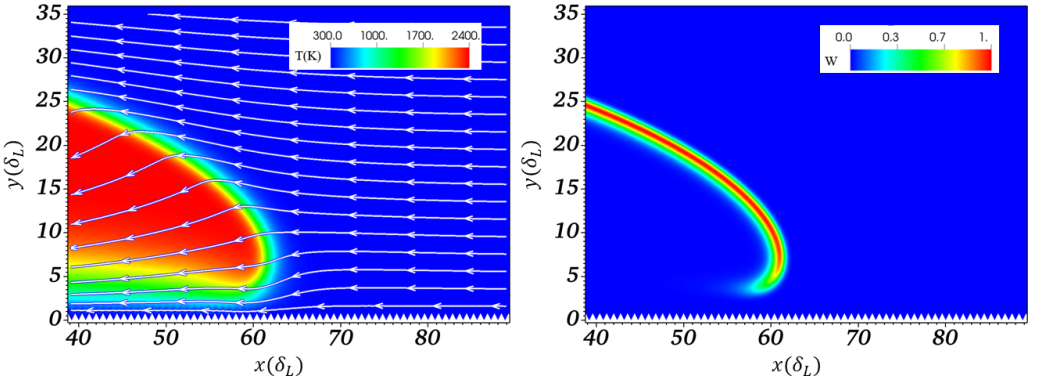

FIG. 9. (Left) Temperature field and streamlines, and (right) scaled reaction rate field, under critical condition. Isothermal wall, $\Theta = 8$, $g = \frac{dU}{dy} = 0.1564 S_L/\delta_L$, $k = 4$.

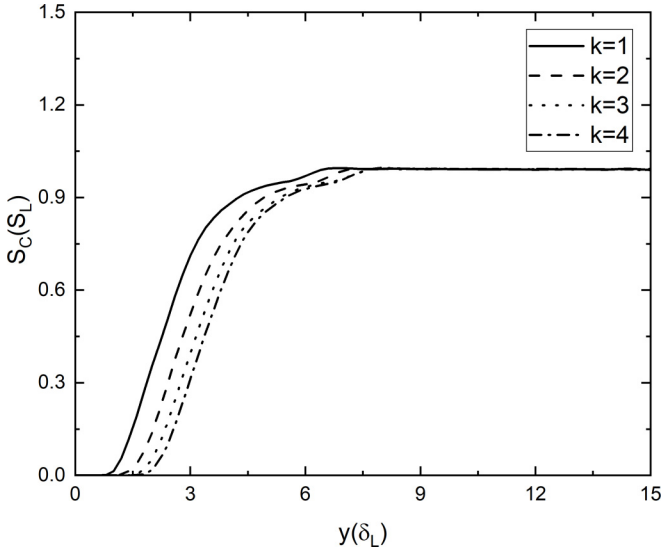

FIG. 10. Radial profile of consumption speed at different roughness slopes k, for $\Theta = 8$, $g = \frac{dU}{dy} = 0.1S_L/\delta_L$.

rather something in between; therefore the present study is mainly aimed at investigating the limit cases of the influence of thermal boundary conditions on flashback, with isothermal walls assumed to be more realistic as compared to adiabatic ones.

Next, we consider the four cases ($k = 1,2,3,4$) with the inlet velocity gradient set at $0.1S_L/\delta_L$, which is smaller than any critical blowout velocity gradient, and $\Theta = 8$ (same set of parameters as in Fig. 6). Figure 10 shows the profiles of the consumption speed $S_c(y)$ in the radial direction (along the y axis). The consumption speed profile $S_c(y)$ is calculated by integration of the reaction rate in the direction normal with respect to the flame front. The results of Fig. 10 confirm that, as the roughness slope k increases, the increased heat loss to the wall roughness elements indeed modifies the penetration distance, and, therefore, it may slow the flame down (in laboratory frame) and decrease the critical velocity gradient, thus lowering the risk of boundary layer flashback.

By extracting the flow velocity profile upstream of the flame surface (beyond the flow reversal area, at the distance of approximately $50\delta_L$ ahead of the flame tip) and comparing it to the consumption speed profile $S_c(y)$, we can assess the performance of the critical gradient model [2] in the case of a wall with fine roughness. As seen from Fig. 11, the critical gradient model may need additional interpretation when being directly applied to the cases with wall roughness. It is seen that the blowout happens at somewhat lower velocity gradient than predicted by the theory. As roughness modifies both the quenching distance and the flow in the vicinity of the wall, the critical condition is reached more easily as compared to the theory [2].

To provide a more specific explanation to that, a closer look into the flow around the flame is needed. As shown in Fig. 12, the radial velocity profile just in front of the flame tip (extracted at the distance of $2\delta_L$ ahead of the flame tip) is largely modified, which can be attributed to the influence of thermal gas expansion at the flame [8,9]. It is seen that in both cases, the velocity gradient just beneath the flame tip is higher as compared to the original linear velocity profile encountered upstream, which would explain the facilitation of flame blowout. This local modification of the incoming flow profile by the flame is not taken into account in the critical gradient theory [2], where the velocity balance between the consumption speed at the flame surface and nearly linear inlet velocity profile is considered.

Figure 13 shows the comparison of consumption speed profile $S_c(y)$ and the velocity U' extracted along the curved flame front in the vicinity of the flame tip. As seen from Fig. 13, the velocity U'

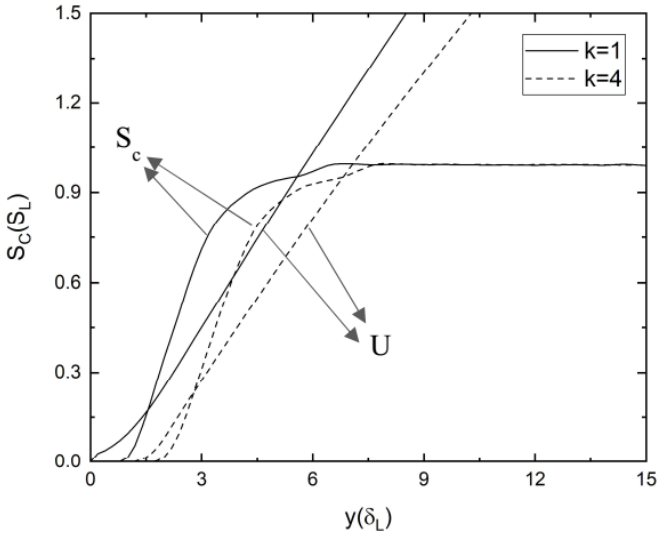

FIG. 11. Comparison of critical gradient model [2] and simulation results for $\Theta = 8$, $g = \frac{dU}{dy} = 0.1 S_L/\delta_L$, $k = 1$, and $k = 4$. S_c is consumption speed profile in the radial direction, U is radial velocity profile ahead of the flame.

becomes equal to S_c at the penetration distance, where $S_c(y)$ reaches its maximum, which somewhat reconciles the present results and Lewis and von Elbe's theory. The result also indicates that the velocity balance for the estimation of the critical condition for flashback should take into account the modifications of the flow by the flame, which is neglected in the classical critical gradient theory [2].

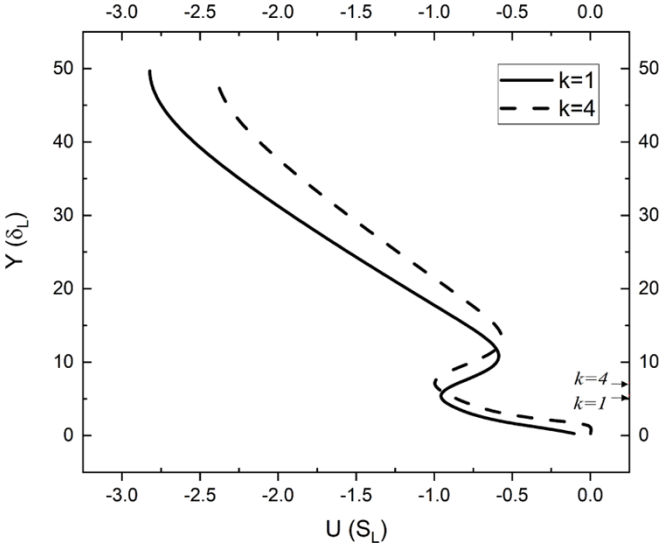

FIG. 12. Radial velocity profile in front of the flame tip for critical conditions, $\Theta = 8$, $k = 1$, and $k = 4$. Arrows show the vertical position of flame tip.

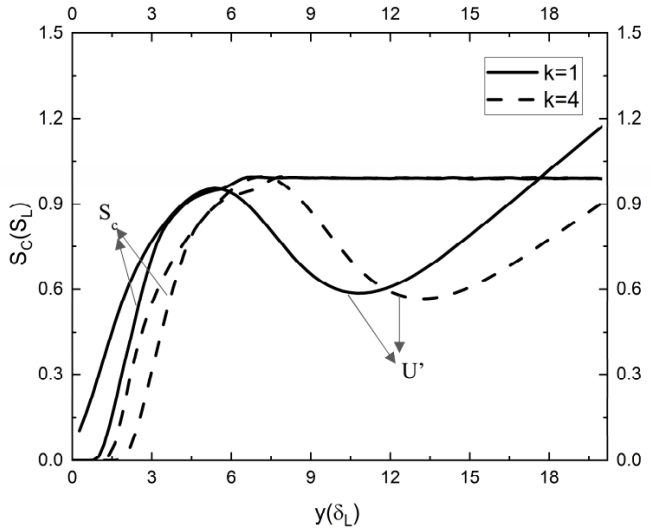

FIG. 13. Comparison of the consumption speed profile $S_c(y)$ and velocity along the curved flame front at critical condition for $\Theta = 8$, $k = 1$, and $k = 4$.

IV. CONCLUSIONS

In this study, the effect of fine wall roughness on the laminar boundary layer flame flashback is investigated numerically for different levels of fine wall roughness, defined by different roughness element heights for a given roughness base size, and for different thermal expansions. It is shown that the rough boundary has a non-negligible influence on the boundary layer flashback. On one hand, the larger roughness level modifies the flow field through forming the thicker flow stagnation zone in the near-wall region. On the other hand, larger roughness level also results in a larger heat loss, which increases the quenching gap near the wall, as well as penetration distance (as defined by Lewis and von Elbe), and, consequently, the critical velocity gradients and flame propagation velocities are modified. The critical velocity gradient is shown to decrease with wall roughness level and increase with thermal expansion ratio. By comparing the simulations with heat loss at the wall to the auxiliary simulations with adiabatic walls, we conclude that the modification of the heat loss intensity by the increasing wall roughness level may be more important than the modification of oncoming flow when the thermal resistance of the wall is low (e.g., in the case of metal walls). For the walls with heat losses, the flame propagation velocity (in the laboratory frame) is found to decrease with roughness. By investigating the critical conditions for the flame flashback, it is shown that the oncoming flow profile is largely modified in the vicinity of the flame, which is neglected by the classic critical gradient theory. A velocity balance can be formulated by taking the flow deformation by the flame into account.

ACKNOWLEDGMENTS

We thank Florian Schmidt for the help with computations, and Hongtao Zhong for useful discussions. The work is sponsored by the National Natural Science Foundation of China (NSFC) through Grant No. 51750110503, by the State Key Laboratory of Explosion Science and Technology (Beijing Institute of Technology) through Opening Project No. KFJJ21-10M, and by start-up funding from Tsinghua University. Pilot computations and data handling were enabled by resources provided by the Swedish National Infrastructure for Computing (SNIC) at High Performance Computing Center North (HPC2N) partially funded by the Swedish Research Council through Grant Agreement No. 2018-05973.

[1] A. Kalantari and V. McDonell, Boundary layer flashback of non-swirling premixed flames: Mechanisms, fundamental research, and recent advances, Prog. Energy Combust. Sci. **61**, 249 (2017).
[2] B. Lewis and G. von Elbe, Stability and structure of burner flames, J. Chem. Phys. **11**, 75 (1943).
[3] S. T. Lee and J. S. T'ien, A numerical analysis of flame flashback in a premixed laminar system, Combust. Flame **48**, 273 (1982).
[4] A. A. Putnam and R. A. Jensen, Application of dimensionless numbers to flash-back and other combustion phenomena, Symp. Combust. Flame Explos. Phenom. **3**, 89 (1948).
[5] V. Kurdyumov, E. Fernandez, and A. Linan, Flame flashback and propagation of premixed flames near a wall, Proc. Combust. Inst. **28**, 1883 (2000).
[6] V. Kurdyumov, E. Fernández-Tarrazo, J. M. Truffaut, J. Quinard, A. Wangher, and G. Searby, Experimental and numerical study of premixed flame flashback, Proc. Combust. Inst. **31**, 1275 (2007).
[7] C. Eichler and T. Sattelmayer, Experiments on flame flashback in a quasi-2D turbulent wall boundary layer for premixed methane-hydrogen-air mixtures, J. Eng. Gas Turbines Power **133**, 1093 (2011).
[8] A. Gruber, J. H. Chen, D. Valiev, and C. K. Law, Direct numerical simulation of premixed flame boundary layer flashback in turbulent channel flow, J. Fluid Mech. **709**, 516 (2012).
[9] A. Gruber, A. R. Kerstein, D. Valiev, C. K. Law, H. Kolla, and J. H. Chen, Modeling of mean flame shape during premixed flame flashback in turbulent boundary layers, Proc. Combust. Inst. **35**, 1485 (2015).
[10] A. Gruber, E. S. Richardson, K. Aditya, and J. H. Chen, Direct numerical simulations of premixed and stratified flame propagation in turbulent channel flow, Phys. Rev. Fluids **3**, 110507 (2018).
[11] D. Ebi and N. Clemens, Experimental investigation of upstream flame propagation during boundary layer flashback of swirl flames, Combust. Flame **168**, 39 (2016).
[12] C. Eichler, G. Baumgartner, and T. Sattelmayer, Experimental investigation of turbulent boundary layer flashback limits for premixed hydrogen-air flames confined in ducts, J. Eng. Gas Turbines Power **134**, 011502 (2012).
[13] Y. Wakisaka, M. Inayoshi, K. Fukui, H. Kosaka, Y. Hotta, A. Kawaguchi, and N. Takada, Reduction of heat loss and improvement of thermal efficiency by application of "temperature swing" insulation to direct-injection diesel engines, SAE Int. J. Engines **9**, 1449 (2016).
[14] B. Zhang, The influence of wall roughness on detonation limits in hydrogen–oxygen mixture, Combust. Flame **169**, 333 (2016).
[15] M. Al-Fahham, A modelling and experimental study to reduce boundary layer flashback with microstructure, Ph.D. thesis, Cardiff University, 2017.
[16] F. A. Hatem, A. S. Alsaegh, M. Al-Faham, A. Valera-Medina, C. T. Chong, and S. M. Hassoni, Enhancing flame flashback resistance against combustion induced vortex breakdown and boundary layer flashback in swirl burners, Appl. Energy **230**, 946 (2018).
[17] E. O.Tuck and A. Kouzoubov, A laminar roughness boundary condition, J. Fluid Mech. **300**, 59 (1995).
[18] M. B. Turgay and A. G. Yazicioglu, Effect of surface roughness in parallel plate microchannels on heat transfer, Numer. Heat Transfer, Part A **56**, 497 (2009).
[19] D. Valiev, V. Bychkov, V. Akkerman, L.-E. Eriksson, and M. Marklund, Heating of the fuel mixture due to viscous stress ahead of accelerating flames in deflagration-to-detonation transition, Phys. Lett. A **372**, 4850 (2008).
[20] D. M. Valiev, V. Bychkov, V. Akkerman, L.-E. Eriksson, and C. K. Law, Quasi-steady stages in the process of premixed flame acceleration in narrow channels, Phys. Fluids, **25**, 096101 (2013).
[21] A. Adebiyi, O. Abidakun, G. Idowu, D. Valiev, and V. Akkerman, Analysis of nonequidiffusive premixed flames in obstructed channels, Phys. Rev. Fluids **4**, 063201 (2019).
[22] N. Andersson, L.-E. Eriksson, and L. Davidson, Investigation of an isothermal Mach 0.75 jet and its radiated sound using large-eddy simulation and Kirchhoff surface integration, Int. J. Heat Fluid Flow **26**, 393 (2005).
[23] C. Wollblad, L. Davidson, and L.-E. Eriksson, Large eddy simulation of transonic flow with shock wave/turbulent boundary layer interaction, AIAA J. **44**, 2340 (2006).
[24] Z. Duan, B. Shaffer, V. McDonell, G. Baumgartner, and T. Sattelmayer, Influence of burner material, tip temperature, and geometrical flame configuration on flashback propensity of H_2-air jet flames, J. Eng. Gas Turbines Power **136**, 021502 (2014).

[25] R. Feng, A. Gruber, J. H. Chen, and D. M. Valiev, Influence of gas expansion on the propagation of a premixed flame in a spatially periodic shear flow, Combust. Flame **227**, 421 (2021).

[26] B. Boust, J. Sotton, S. A. Labuda, and M. Bellenoue, A thermal formulation for single-wall quenching of transient laminar flames, Combust. Flame **149**, 286 (2007).